31. I. Yu. Brailovskaya, "Method of solution of problems with strong viscous interaction," Dokl. Akad. Nauk SSSR, 162, No. 1 (1965).
32. V. N. Varapaev, "Numerical study of periodic jet flow of a viscous incompressible fluid," Izv. Akad. Nauk SSSR, Mekh. Zhidk. Gaza, No. 3 (1968).

ENTRAINED DOWNWARD FLOW OF A GAS AND A LIQUID IN A VERTICAL CHANNEL

V. V. Lozovetskii

UDC 532.529.5

The fluid friction and breakaway of liquid from the surface of a film are investigated and described quantitatively.

Relatively few investigations have been devoted to the interaction of gas and liquid flows in downward and upward entrained motion [1-6]. This type of flow takes place in various heat- and mass-transfer devices and permits appreciable intensification of heat-transfer processes at a solid — liquid interface as well as mass-transfer processes at a liquid — gas interface. The efficiency of heat- and mass-transfer equipment is improved in this case by the reduced film thickness and increased velocity in the film under the action of the gas flow and inception of turbulence in the gas layers adjacent to the film surface, all of which intensify heat and mass transfer at the liquid — gas interface.

The annular-mist flow regime covered by the results of the investigation described below is observed at high velocities and large volume contents of the gaseous phase. It is characterized by two sharply differentiated flow zones: 1) the wall zone, which is occupied by a thin liquid film; 2) the flow core, in which the gaseous phase moves together with suspended droplets of the liquid phase, which are broken away from the surface of the film. The velocity of the film is much lower than that of the gas. Mass transfer takes place between the film and the core, further intensifying the heat- and mass-transfer processes and simultaneously increasing the fluid-friction (viscous) losses.

We have investigated the mass transfer and fluid friction associated with entrained downward flow of a liquid film and gas core on an experimental setup consisting of a working section in the form of a vertical transparent plastic pipe of inside diameter $d = 40$ mm and length $l = 2000$ mm. In the upper part of the working section we installed a film-forming device in the form of an annular injection slot of width 0.6 mm, along with an air-injection device comprising a Vitoshinskii nozzle, which provides a uniform gas-velocity profile in the entry section. The investigations were carried out for a gas — liquid system with water and air under isothermal conditions.

The water entered a supply tank, in which an overflow pipe was installed to maintain a constant level, thus assuring a constant flow rate throughout one experiment. From the supply tank the water flowed into the film-forming device. The static pressure was tapped at distances of 35, 895, and 1915 mm from the entry of water and air into the working section, making it possible to determine the pressure drops along the length of the channel.

A chamber was placed in the lower part of the working section to permit separation of the liquid streaming along the pipe wall as a film and the flow core of air containing suspended detached liquid droplets. The latter were captured by cylindrical sampling probes with diameters $d_i = 10$, 20, 30, and 35 mm, which were mounted at a distance of 2000 mm from the entry to the working section and subsequently delivered their contents into the measurement vessel.

The mass-flow of water in the experiments was $(1.54 \text{ to } 12.56) \cdot 10^{-2}$ kg/sec, corresponding to a variation of the spray density Γ from 0.125 to 1.6 kg/m · sec. The water temperature in this case was 8 to 12°C, and the Reynolds number of the liquid had values

N. É. Bauman Moscow Higher Technical School. Translated from Inzhenerno-Fizicheskii Zhurnal, Vol. 35, No. 2, pp. 313-319, August, 1978. Original article submitted July 19, 1977.

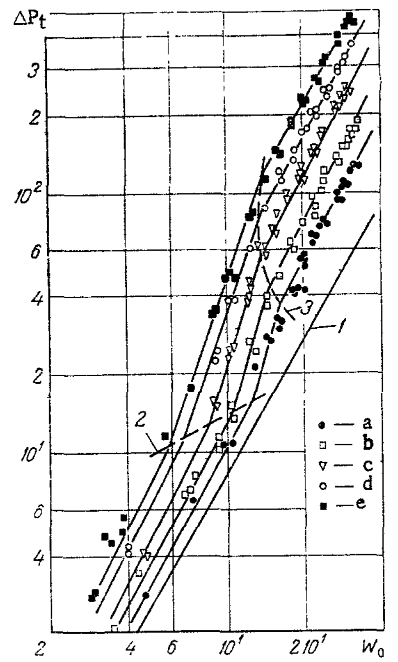

Fig. 1

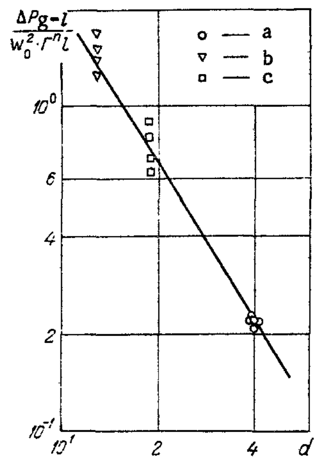

Fig. 2

Fig. 1. Total pressure drop ΔP_t, mm H_2O, versus relative airflow velocity W_0, m/sec. 1) According to Eq. (6); 2) end of phase-separated flow regime; 3) beginning of regime of strong breakaway and entrainment of liquid; a) $\Gamma = 0.124$ kg/m · sec; b) 0.25; c) 0.5; d) 1.0; e) 1.6 kg/m · sec.

Fig. 2. Hydrodynamic losses versus droplet diameter d, mm, calculated according to (8) and (9) (solid line) and experimental: a) present study, d = 40 mm; b) data of [2], d = 13 ± 0.1 mm; c) data of [3], d = 18.7 mm.

$$\mathrm{Re}_\delta = \frac{\Gamma}{\mu_l} = 100 - 1260. \tag{1}$$

This range of Reynolds numbers corresponds to both laminar-ripple and turbulent flow of the liquid film.

The mass flow of gas $G_g = 0.008$–0.06 kg/sec, corresponding to a variation of the reduced Reynolds number of air

$$\mathrm{Re}_g = \frac{4G_g}{\pi d \mu_g} = (1.2\text{—}10.0)\cdot 10^4. \tag{2}$$

The air temperature was maintained equal to the water temperature. This condition ensured isothermicity throughout the experiments. In determining the mean air velocity W_g we took into account the reduction in the throughflow cross section of air due to the presence of the liquid film flowing along the inner surface of the vertical channel. All processing of the experimental data was carried out for the mean relative gas velocity W_0, defined as

$$W_0 = W_g - W_l, \tag{3}$$

where W_g is the mean air velocity, m/sec, given by the expression

$$W_g = 4G_g/\gamma_g \pi d, \tag{4}$$

and W_l is the mass-flow-mean velocity of the liquid in the film, m/sec:

$$W_l = G_l/\gamma_l \pi d\delta. \tag{5}$$

The relative air velocity varied during the experiments in the interval 3.6 m/sec $\leq W_0 \leq$ 32.5 m/sec.

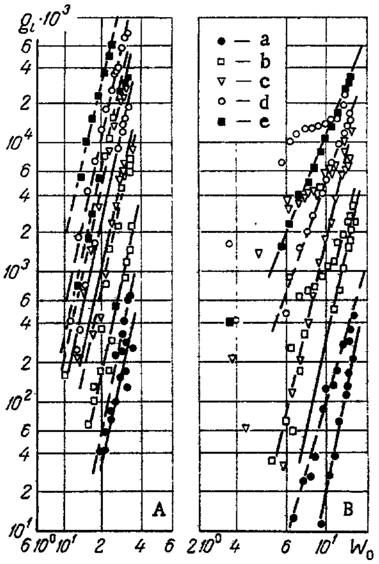

Fig. 3

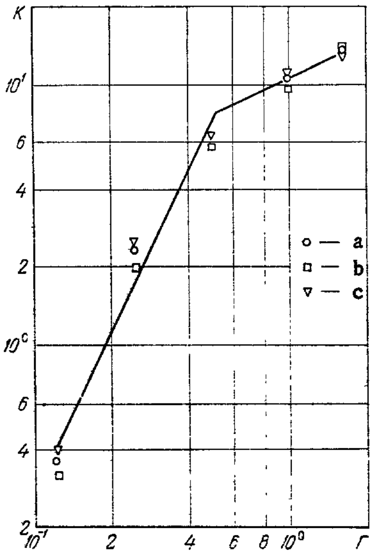

Fig. 4

Fig. 3. Quantity of liquid g_l, g/sec, detached from film surface versus relative air velocity W_0, m/sec. A) $d_p = 10$ mm (solid lines) and $d_p = 20$ mm (dashed lines); B) $d_p = 30$ mm (solid) and $d_p = 35$ mm (dashed). The rest of the notation is the same as Fig. 1.

Fig. 4. Quantity $K = g_l \cdot 10^8 / G_l W_0^{4.5} \xi^{2.4}$ versus spray density Γ, kg/m · sec. a) $\xi = 0.25$; b) 0.5; c) 0.75.

The dependence of the hydrodynamic losses on the relative air velocity is given in Fig. 1. An analysis of the curves confirms the existence of two characteristic regimes of downward two-phase flow:

1) pure annular flow, i.e., phase-separated flow;

2) breakaway and entrainment of liquid droplets from the film surface, i.e., annular-mist flow.

The pure annular flow regime is observed for the investigated spray densities at relative air velocities up to 6-12 m/sec. The instant of onset of breakaway (curve 2) depends on the spray density; the higher the value of the latter the smaller will be the air velocities at which liquid begins to break away from the surface of the film.

The annular-mist flow regime is observed, beginning with values of $W_0 > 14$-16 m/sec; this transition is essentially independent of the spray density.

In the interval of relative air velocities $W_0 = 6$-16 m/sec we have a transition flow regime characterized by the maximum pressure gradient, i.e., maximum fluid-friction losses.

Visual observations indicated that for small air velocities the effect of the air on the film is slight. With an increase in the relative air velocity waves appear on the film surface, their amplitude increasing with the relative velocity of the gaseous phase. Sliding ripple waves appear, possessing the maximum amplitude and velocity. At the critical air velocity the disturbing forces of the air at the tips of the wave crests is sufficient to detach liquid droplets, which are entrained by the air flow and dispersed throughout its cross section.

It is well known [2] that the total pressure drop for downward two-phase flow is determined as the sum of the expenditure of energy of the gas in dry friction in the pipe ΔP_{fr} and the expenditure of energy of the gas in friction against the liquid film, breakaway of droplets from its surface, and acceleration of the droplets in the flow core, ΔP_{g-l}. The dry-friction losses (curve 1 in Fig. 1) can be determined from the standard formula

$$\Delta P_{fr} = \lambda \frac{l}{d} \frac{\gamma g W_0}{2g}, \tag{6}$$

in which the friction coefficient λ is determined according to Blasius and for $Re_g \leq 10^5$

$$\lambda = 0.316 / Re_g^{0.25}. \tag{7}$$

The energy expenditures in friction against the liquid film, breakaway of droplets from its surface, and acceleration of the droplets are defined as $\Delta P_{g-l} = \Delta P_t - \Delta P_{fr}$. An analysis of the data in Fig. 1 shows that for the breakaway–entrainment regime $\Delta P_{g-l} \sim W_0^2$. In phase-separated flow $\Delta P_{g-l} \sim W_0^{1.75}$; i.e., the air velocity affects ΔP_{g-l} to the same degree as for the dry pipe. These data are consistent with earlier results [2]. For $\Gamma \leq 0.5$ kg/m · sec, corresponding to $Re_\delta \leq$ 385-400, i.e., laminar film flow, $\Delta P_{g-l} \sim \Gamma^{0.88}$. For $\Gamma > 0.5$ kg/m · sec, i.e., for turbulent film flow, the power exponent is slightly different: $\Delta P_{g-l} \sim \Gamma^{0.72}$.

The subsequent processing of the experimental data was carried out in coordinates $\Delta P_{g-l} = f(W_0;\ \Gamma;\ l/d)$. The following relations were obtained as a result for determining the values of ΔP_{g-l}:

$$\Delta P_{g-l} = 79.8 W_0^2 \Gamma^{0.88} \frac{l}{d^{1.6}} \tag{8}$$

for $\Gamma \leq 0.5$ kg/m · sec;

$$\Delta P_{g-l} = 68 W_0^2 \Gamma^{0.72} \frac{l}{d^{1.6}} \tag{9}$$

for $\Gamma > 0.5$ kg/m · sec.

These expressions are applicable only for the breakaway–entrainment regime, i.e., for $W_0 = 14$-16 m/sec. The scatter of the experimental points and of the experimental data published in [2, 3] relative to the curves calculated according to relations (8) and (9) does not exceed ±20% (Fig. 2). Figure 2 gives a compilation of the experimental data obtained by various authors in working sections of various diameters, providing a means for assessing the influence of the diameter on the hydrodynamic losses.

Besides the determination of the foregoing quantities, equally important in two-phase flow is the quantitative description of the breakaway and entrainment of droplets from the surface. By taking into account the breakaway of liquid in the core it is possible to determine more precisely the local characteristics of the film and the heat- and mass-transfer coefficients. Some authors have published [3-5] a qualitative description of the breakaway process in downward annular-mist flow. However, the complexity of any theoretical analysis of the breakaway process and the lack of sufficient experimental data have so far precluded the existence of quantitative relations describing the process.

As mentioned, with an increase in the air velocity the pure annular flow regime is eventually superseded by annular-mist flow. As the relative air velocity is further increased the pulsating ripple motion on the surface is intensified, causing the quantity of detached liquid to increase. According to Didenko and others [6], the critical air velocity characterizing the beginning of breakaway depends weakly on the dimensions and orientation of the channel. It has been confirmed experimentally [4] that at a sufficient distance from the entry of liquid into the working section ($l/d > 50$) the two-phase flow may be regarded as steady. The quantities of liquid detached from the film surface and precipitated into the film from the core are equal in this case. It is under such conditions that the experiments described here were conducted.

Figure 3 gives the dependence of the quantity g_i of liquid captured by the sampling probe on the relative air velocity W_0 for various spray densities and sampling-probe diameters. An analysis of the curves shows that for probes with diameters of 10 and 20 mm, irrespective of the spray density, $g_i \sim W_0^{4.5}$. We obtain the same result for a probe diameter of 30 mm, but only for $\Gamma \leq 0.5$ kg/m · sec, corresponding to film Reynolds numbers $Re_\delta \leq$ 385-400, For $\Gamma > 0.5$ kg/m · sec, i.e., for $Re_\delta > 400$, corresponding to turbulent film flow, the power of W_0 differs. For probes with a diameter of 35 mm the dependence of the quantity of detached liquid on the relative air velocity has a more complex behavior. This fact is attributable to capture of the wave crests by the sampling probe. The presence of a horizontal plateau in the interval of relative air velocities from 10 to 20 m/sec for a probe of diameter 35 mm can be explained by the fact that the main contribution to the quantity of liquid entrained by the probe is from liquid at the crests of waves that have the maximum value for the indicated values of the relative air velocity, according to [1, 3], and overlap the space between the inner surface of the channel and the probe; this space is equal to 2.5 mm. It is probably for this reason the probe with diameter of 30 mm also exhibits a deviation for $\Gamma > 0.5$ kg/m · sec.

In the core of the gas — liquid flow we discern two zones, which differ in the value of the flux density of detached liquid $g_l = (g_i - g_{i-1})/(F_i - F_{i-1})$, where $(g_i - g_{i-1})$, g/sec, is the quantity of liquid flowing across an annular area $(F_i - F_{i-1})$, m^2:

a) the central zone of the core $0 \leq d_p/d \leq 0.75$, in which g_l is approximately constant;

b) the zone adjacent to the surface of the film $0.75 \leq d_p/d \leq 0.875$, in which the liquid flowing in the film, specifically at the wave crests, makes a significant contribution to the value of g_l.

For equal spray density, with an increase in the relative air velocity the flux density of detached liquid in the central part of the channel increases. A similar result is obtained when Γ is increased with W_0 = const. Increasing Γ or W_0 tends to equalize the distribution of detached liquid in the channel cross section.

The subsequent processing of experimental data to determine the quantity of detached liquid was carried out in coordinates

$$g_i/G_l = f(W_0;\ \Gamma;\ \xi) \tag{10}$$

for the interval $0 \leq \xi \leq 0.75$.

The results of this processing show that for laminar-ripple flow the quantity $g_i/W_0^{4.5}\xi^{2.4}G_l$ is proportional to $\Gamma^{2.04}$, and for turbulent flow it is proportional to $\Gamma^{0.461}$ (Fig. 4). On this basis we obtain the following relations for the quantity of detached liquid and its radial distribution in the channel:

$$g_i/G_l = 0.28 \cdot 10^{-6}\,\Gamma^{2.04}\,W_0^{4.5}\,\xi^{2.4} \tag{11}$$

for $\Gamma \leq 0.5$ kg/m · sec, i.e., for $Re_\delta < 400$;

$$g_i/G_l = 0.1 \cdot 10^{-6}\,\Gamma^{0.46}\,W_0^{4.5}\,\xi^{2.4} \tag{12}$$

for $\Gamma > 0.5$ kg/m · sec.

Relations (11) and (12) were obtained for the regime of breakaway and entrainment of liquid from the film surface, i.e., for $W_0 > 14$-16 m/sec, and well generalize the experimental data in the interval $0 \leq \xi \leq 0.75$ for $l/d = 50$. The maximum scatter of the experimental points relative to the generalizing curves is not greater than ±20%. The maximum deviations in this case are observed for $\Gamma < 0.256$ kg/m · sec.

NOTATION

d_p, diameter of sampling probe; Γ, spray density; G_l, initial mass-flow rate of liquid in film; Re_δ, Reynolds number of liquid film; μ_l, dynamic viscosity of water; G_g, mass-flow rate of gas (air); d, diameter of working section; W_g, mass-flow-mean velocity of air; W_l, mass-flow-mean velocity of liquid film; W_0, mean relative air velocity; γ_g, density of air; ΔP_{fr}, energy losses of gas in dry friction in pipe; ΔP_{g-l}, energy losses of gas in breakaway of liquid droplets from film surface and their acceleration; ΔP_t, total energy losses of gas; λ, fluid friction coefficient; l, length of working section; g_i, quantity of liquid from flow core entering a sampling probe of the i-th diameter; g_l, flux density of detached liquid in flow core; F_i, inside area of i-th sampling probe; ξ, dimensionless radial coordinate.

LITERATURE CITED

1. Sze-Foo Chien and W. Ibele, "Pressure drop and liquid film thickness of two-phase annular and annular-mist flows," Trans. ASME, Ser. C: J. Heat Transfer, 86, No. 1 (1964).
2. L. Ya. Zhivaikin and B. P. Volgin, "Fluid friction in downward two-phase flow in film equipment," Zh. Prikl. Khim., No. 6 (1963).
3. I. N. Paleev, F. A. Agafonova, M. E. Lavrent'ev, and K. P. Malyus-Nalitskii, "Flow in the core of annular-mist gas — liquid flow," Energomashinostroenie, No. 3 (1966).
4. A. Ya. Didenko et al., "Local characteristics of isothermal two-phase flow," in: Thermophysical Problems of Nuclear Reactors [in Russian], No. 2 (V. I. Petrovich, editor), Atomizdat, Moscow (1969).
5. A. D. Didenko et al., "Central zone of an annular-mist water — airflow," in: Thermophysical Problems of Nuclear Reactors [in Russian], No. 3 (V. I. Subbotin, editor), Atomizdat, Moscow (1971).
6. G. B. Wallis, One-Dimensional Two-Phase Flow, McGraw-Hill, New York (1969).